Phospholipid—polymer amphiphile hybrid assemblies and their interaction with macrophages

Karthiga Panneerselvam,[1,a)] Martin E. Lynge,[1,a)] Camilla Frich Riber,[2,a)] Sofia Mena-Hernando,[1] Anton A. A. Smith,[2] Kenneth N. Goldie,[3] Alexander N. Zelikin,[1,2] and Brigitte Städler[1,b)]
[1]*Aarhus University, Interdisciplinary Nanoscience Center (iNANO), Aarhus, Denmark*
[2]*Department of Chemistry, Aarhus University, Aarhus, Denmark*
[3]*Center for Cellular Imaging and Nano Analytics, Biozentrum, University of Basel, Basel, Switzerland*

(Received 13 May 2015; accepted 11 August 2015; published online 24 August 2015)

Recently, the combination of lipids and block copolymers has become an alternative to liposomes and polymersomes as nano-sized drug carriers. We synthesize novel block copolymers consisting of poly(cholesteryl acrylate) as the hydrophobic core and poly(*N*-isopropylacrylamide) (PNIPAAm) as the hydrophilic extensions. Their successful phospholipid-assisted assembly into vesicles is demonstrated using the evaporation-hydration method. The preserved thermo-responsive property of the lipid-polymer hybrids is shown by a temperature dependent adsorption behaviour of the vesicles to poly(L lysine) coated surfaces. As expected, the vesicle adsorption is found to be higher at elevated temperatures. The cellular uptake efficiency of hybrids is assessed using macrophages with applied shear stress. The amount of adhering macrophages is affected by the time and level of applied shear stress. Further, it is found that shorter PNIPAAm extensions lead to higher uptake of the assemblies by the macrophages with applied shear stress. No inherent cytotoxicity is observed at the tested conditions. Taken together, this first example of responsive lipid-polymer hybrids, and their positive biological evaluation makes them promising nano-sized drug carrier candidates. © *2015 AIP Publishing LLC*. [http://dx.doi.org/10.1063/1.4929405]

I. INTRODUCTION

Nano-sized drug carriers in the form of micelles,[1] polymersomes,[2] or liposomes[3] are widely considered for drug delivery applications. Each of these platforms has its own advantages but they are also not devoid of shortcomings. Lipids are natural building blocks, and assemblies thereof—liposomes—are inherently biocompatible. Other advantages of liposomes are their formation via self-assembly, and the loading with hydrophilic and/or hydrophobic cargo is straightforward and amenable for automation.[4] From a practical standpoint, assembly of liposomes through hydration of thin lipid films followed by extrusion or inkjet printing of the lipid solution[5] allows for controlling their size. However, compared to their polymer-based counterpart, liposomes suffer from instability in biological fluids. In turn, assembly of amphiphilic (co)polymers into polymersomes is also an entropy-driven process, with the final size and morphology of the supramolecular assembly dependent on the macromolecular characteristics of the polymer, specifically the volume fractions of the two blocks.[6] Recent advances in modern polymer chemistry allow for tailoring of the polymersomes' morphology and biomedical properties through rational design of the building blocks, their relative size, etc., as recently reviewed by LoPresti *et al.*[7] and Rösler *et al.*[8] However, the tailor-made polymer building blocks may not be fully decisive on the success of the self-assembly, and technological

[a)]K. Panneerselvam, M. E. Lynge, and C. F. Riber contributed equally to this work.
[b)]bstadler@inano.au.dk

considerations are also important such as the method employed for the assembly (solvent exchange, microfluidics, etc.). Regretfully, for the overall majority of the polymers, hydration of dried polymer films does not yield polymersomes and extrusion may be problematic if performed at room temperature, which is considerably lower than the glass transition temperature for most hydrophobic polymers employed in the design of polymersomes.

In the past few years, the combination of lipids and block copolymers has been considered to overcome the outlined challenges while preserving the advantages of the individual building blocks as recently reviewed by Le Meins *et al.*[9] Mixed films formed by block copolymers and lipids are suitable for hydration-based assembly of supramolecular associates—opening up broad opportunities for facile assembly. Furthermore, incorporated lipids are poised to act as lubricants and allow for extrusion to control the size. Finally, co-assembly of lipids and polymers may be a straightforward approach to form hybrid lipid-polymer supramolecular associates with engineered properties such as temperature responsiveness. Block copolymers with poly (dimethyl siloxane),[10,11] poly(isobutylene),[12,13] poly(butadiene),[14–17] or poly(ε-caprolactone)[18] as the hydrophobic block and poly(ethylene glycol) (PEG) or poly(2-methyloxazoline) as the hydrophilic blocks in combination with different lipids were so far considered in this context. The focus of these reports was placed on the physical-chemical characterization of the hybrid assemblies. The solitary biological evaluation of such hybrid assemblies was that by Cheng *et al.* who demonstrated that the use of hybrid structures could significantly improve the efficiency of cell surface receptor targeting.[15] The potential of hybrid lipid-polymer assemblies for biomedical applications therefore remains largely unexplored.

From a different perspective, over the past few years, a move towards investigating interactions of nano-sized drug carriers with mammalian cells with applied shear stress created by the flow of cell culture media over the cells has been observed, especially when considering endothelial cells.[19–24] There is a growing understanding in the field that static cell culture neglects effects arising from shear stress—whereas these considerations are often more than minor in the context of drug delivery as recently reviewed by Godoy-Gallardo *et al.*[25] For instance, we have recently shown that the intracellular delivery of model compounds was significantly enhanced with applied shear stress.[26,27] Apart from the predominantly employed endothelial cells, which line our blood vessels and are therefore permanently exposed to blood flow induced shear stress, macrophages are important to investigate in this context. Circulating macrophages are also exposed to mechanical stimuli induced by flow. On the other hand, tissue resident macrophages, e.g., Kupffer cells, the liver resident macrophages, are important cells in the context of drug delivery. However, only very few reports investigated the uptake of cargo by macrophages with applied shear stress.[28–30] An interesting result in this context is the observation that the endocytic uptake of the factor VIII-von Willebrand factor complex by macrophages required applied shear stress in the range of 4 dyn cm^{-2} and above.[29]

Herein, we report the assembly and characterization of lipid-polymer hybrid supramolecular carriers based on zwitterionic phospholipids and block copolymers with poly(cholesteryl acrylate) (PChA) as the hydrophobic core and poly(*N*-isopropylacrylamide) (PNIPAAm) as hydrophilic extensions, and characterize the uptake of these potential drug carriers by macrophages with applied shear stress (Scheme 1). Specifically, we (i) synthesized a selection of novel amphiphilic ABA block copolymers with varying lengths of both hydrophobic and hydrophilic blocks via controlled Reversible Addition-Fragmentation chain Transfer (RAFT) polymerization with a PChA core and either PNIPAAm or poly(poly(ethylene glycol) acrylate) (PEGA) as extensions, (ii) assembled lipid-polymer hybrids with varying composition, (iii) compared the temperature dependent adsorption of these hybrids to poly(L lysine) (PLL) coated surfaces, and (iv) assessed the interaction of these hybrids with macrophages in static conditions and with applied shear stress.

II. EXPERIMENTAL SECTION

A. Materials

Chemicals purchased from Sigma-Aldrich were used as received without purification, unless noted otherwise. Tris(hydroxymethyl)aminomethane (TRIS), sodium chloride (NaCl),

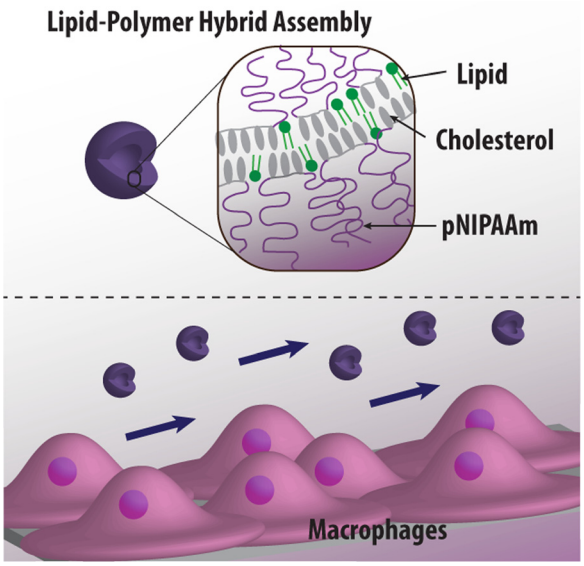

SCHEME 1. Schematic illustration of lipid-polymer hybrid assemblies and their interaction with macrophages with applied shear stress. The employed block copolymer consists of a hydrophobic PChA core and two hydrophilic PNIPAAm extensions.

poly(L lysine) (PLL, MW 40–60 kDa), ethanol, chloroform (purity $\geq$ 99.5%), cholesterol, butanediol, carbon disulfide, dimethyl 2,6-bromoheptanedioate, poly(ethylene glycol) methyl ether acrylate $M_n \sim 480$ (PEGA), *N*-Isopropylacrylamide (NIPAAm), 2,2′-Azobis(2-methylpropionitrile) (AIBN), trioxane, and common organic solvents were purchased from Sigma-Aldrich. PEGA (M_n 480) was filtered through alumina before use. The zwitterionic lipids 1,2-dioleoyl-*sn*-glycero-3-phosphocholine (DOPC) and fluorescent lipids 1-oleoyl-2-[6-[(7-nitro-2–1,3-benzoxadiazol-4-yl)amino]hexanoyl]-*sn*-glycero-3-phosphocholine (NBD-PC) were purchased from Avanti Polar Lipids, USA.

TRIS buffer was used throughout all experiments consisting of 10 mM TRIS and 150 mM NaCl (pH 7.4). The buffer solutions were made with ultrapure water (Milli-Q gradient A 10 system, resistance 18 MΩ cm, TOC < 4 ppb, Millipore Corporation, USA).

Proton nuclear magnetic resonance (^{1}H-NMR):

^{1}H-NMR spectra were recorded on a Varian Mercury 400 MHz spectrometer. Spectra were referenced to the residual solvent peak, $CDCl^3$ (δ 7.26 ppm).

Gel permeation chromatography (GPC):

Size-exclusion chromatography was performed using a system comprising a LC-20AD Shimadzu HPLC pump, a Shimadzu RID-10A refractive index detector and a DAWN HELEOS 8 light scattering detector along with a SPD-M20A PDA detector, equipped with a Mz-Gel SDplus. Linear column with 5 μm particles length of 300 mm and an internal diameter of 8 mm from MZ-Analysentechnik provide an effective molecular weight range of 10^3–10^6 Da. The eluent was tetrahydrofuran (THF) 30 °C (flow rate: 1 ml min^{-1}).

B. Synthesis and characterization of block copolymers

1. RAFT agent synthesis

The RAFT agent was synthesized using a general procedure previously published.[31] Butanethiol (0.26 ml, 2.41 mmol, 1 eq.), carbon disulfide (0.29 ml, 4.81 mmol, 2 eq.), and chloroform (1.9 ml) were added to a round bottom flask. Triethylamine (0.67 ml, 4.81 mmol, 2 eq.) was added dropwise and the reaction mixture was stirred at room temperature for 40 h. Dimethyl 2,6-bromoheptanedioate (0.25 ml, 1.14 mmol, 0.5 eq.) was added dropwise which caused the mixture to thicken. The reaction mixture was concentrated *in vacuo* and the residue

dissolved in diethylether (10 ml). The solution was washed twice with water, twice with 1 M HCl, twice with water, and twice with brine (approximately 10 ml each time). The solution was dried over $MgSO_4$ and concentrated *in vacuo* yielding a yellow oil. The product was purified by flash column chromatography (CH_2Cl_2, Rf = 0.53, 0.65), yielding the pure product as a yellow oil (0.16 g, 0.30 mmol, 26%).

^{1}H-NMR (400 MHz, $CDCl^3$) δ(ppm): 4.83 (t, 2 H J = 7.2 Hz, -C**H**-S), 3.74 (s, 6 H, C**H**$_3$O-), 3.36 (t, 4 H, J = 7.3 Hz, -C**H**$_2$-S), 2.09–1.86 (m, 4 H, S-CHC**H**$_2$CH$_2$C**H**$_2$CH-S), 1.73–1.64 (m, 4 H, CH_3CH_2C**H**$_2$CH$_2$-), 1.61–1.51 (m, 2 H, S-CHCH$_2$C**H**$_2$CH$_2$CH-S), 1.49–1.36 (m, 4 H, CH_3C**H**$_2$-), 0.94 (t, 6 H J = 7.2 Hz, C**H**$_3$-)

2. Synthesis of cholesteryl acrylate (ChA)

Cholesterol (2.00 g, 5.2 mmol, 1.00 eq.) was dissolved in dichloromethane (10 ml) and triethylamine (5 ml) in a 100 ml round bottom flask. A solution of acryloylchloride (5.65 g, 5.00 ml, 62.40 mmol, 12.00 eq) in dichloromethane (20 ml) was added drop wise to the ice-cooled solution over 30 min. The reaction was monitored by thin layer chromatography. The mixture was concentrated *in vacuo* and purified by precipitation into ethanol (30 ml), filtered, washed with cold ethanol and dried *in vacuo* yielding the pure product as a colorless solid (0.948 g, 2.15 mmol, 41.3%).

3. Synthesis of poly(cholesteryl acrylate) (PChA)

Cholesteryl acrylate (ChA, 2.0 g, 4.5 mmol) and RAFT agent (50 mg, 9.67×10^{-5} mol or 23 mg, 4.54×10^{-5} mol) were combined in an ampule to which azobisisobutyronitrile (AIBN) was added as 200 μl of 7.5 mg ml^{-1} stock solution in toluene (1.5 mg, 9.07×10^{-6} mol), and the mixture was further diluted with toluene to 2.3 ml. The reaction mixture was degassed by 4 freeze–pump–thaw cycles, sealed and then heated at 60 °C in a thermostatted oil bath for 25 h. The resulting polymers were recovered by precipitation into ethyl acetate. Macromolecular characteristics of the polymers are listed in Table II.

4. Synthesis of ABA block copolymers

The two PChA macroRAFT agents (Mn 21 kDa and 40 kDa, $PChA_{21}$ and $PChA_{40}$, respectively) were used to synthesize four different block copolymers using NiPAAM and PEG acrylate as hydrophilic monomers. $PChA_{21}$ was used to obtain copolymers with PEG acrylate and NiPAAM with two varied target molar masses of hydrophilic extensions for the latter; $PChA_{40}$ was used to obtain one block copolymer with NiPAAM with relatively high molar masses of both the centre block and the extensions. In a typical procedure, a stock solution of AIBN, monomer, PChA macro RAFT agent, and trioxane were dissolved in dioxane and toluene (50:50 by volume) in an ampule. Specific quantities of reagents for the four polymerizations are listed in Table I. Four cycles of freeze-pump-thaw were performed following which the ampule was flame-sealed and the polymerization performed at 60 °C for 16 h. Polymers were recovered via precipitation and trituration in water (for PEG acrylate) or methanol (for NiPAAM copolymers). Macromolecular characteristics of the polymers are listed in Table II.

^{1}H-NMR (400 MHz, $CDCl_3$) δ(ppm):

Polymers 1–3 (PChA and NiPAAM) 5.36 (s, 1 H, -C=C**H**-CH$_2$-, PChA), 4.53 (s, 1 H, -C**H**-O-(CO)-, PChA), 4.01 (s, -(CO)-N**H**-CH-, PNIPAM), 3.62–3.35 (bs, PChA aliphatic protons), 2.59–0.49 (broad signal, PChA and PNIPAM aliphatic protons).

Polymer 4 ($PChA_{21}$ and PEG acrylate) 5.36 (s, 1 H, -C=C**H**-CH$_2$-, PChA), 4.53 (s, -C**H**-O-(CO)-, PChA), 4.16 (s, -C**H**$_2$-O-(CO)- PEGA), 3.91–3.29 (bs, PEGA), 2.65–0.50 (broad signal, PChA and PEGA aliphatic protons).

C. Hybrid assembly

Lipid-polymer hybrids were assembled by the evaporation-hydration method. Varying amounts of DOPC lipids (25 mg ml^{-1}, $CHCl_3$) were added to a round-bottom flask. For

TABLE I. Overview over the used amounts and types of chemicals for the synthesis of the block copolymers.

Abbreviation	AIBN	Monomer	Macro RAFT agent
Poly(*N*-isopropylacrylamide)-*b*-poly(cholesteryl acrylate)-*b*-poly(*N*-isopropylacrylamide)			
Polymer 1 (P1)	18 μl,	NIPAAm,	$PChA_{40}$
	3.72 mg ml^{-1} in toluene,	45.6 mg,	83.72 mg,
	4.08×10^{-7} mol	4.03×10^{-4} mol	2.09×10^{-6} mol
Polymer 2 (P2)	20 μl,	NIPAAm,	$PChA_{21}$
	3.24 mg ml^{-1} in toluene,	44.8 mg,	86.30 mg,
	3.95×10^{-7} mol	3.95×10^{-4} mol	4.10×10^{-6} mol
Polymer 3 (P3)	20 μl,	NIPAAm,	$PChA_{21}$
	3.24 mg ml^{-1} in toluene,	24.88 mg,	83.94 mg,
	3.95×10^{-7} mol	2.20×10^{-4} mol	4.00×10^{-6} mol
Poly(poly(ethylene glycol) acrylate)-*b*-poly(cholesteryl acrylate)-*b*-poly(poly(ethylene glycol) acrylate)			
Polymer 4 (P4)	20 μl,	PEGA	$PChA_{21}$
	3.24 mg ml^{-1} in toluene,	353.40 mg,	85.84 mg,
	3.95×10^{-7} mol	7.36×10^{-4} mol	4.09×10^{-6} mol

fluorescent samples, 0.18 mg DOPC lipids were mixed with 100 μl NBD-PC (1 mg ml^{-1}, $CHCl_3$). The chloroform was evaporated followed by the addition of 0.5 ml polymer solution (1 mg ml^{-1}, THF). The THF was removed *in vacuo* for at least 1 h before rehydrating the dried film in TRIS and extrusion through 200 nm filters. Depending on the amount of incorporated polymer, the samples were heated to 42 °C in the latter two steps. For comparison, liposomes were assembled from 0.18 mg DOPC lipids with 0.1 mg NBD-PC, which were dried *in vacuo* for 1 h and rehydrated in TRIS buffer before extrusion through 200 nm filters. Hybrids containing 0.18 mg DOPC lipids and P4 in the same molar lipid/polymer ratio as for P1 were also assembled using the same method. After extrusion, their diameter, polydispersity index (PDI) and ζ-potential were determined by dynamic light scattering (DLS) measurements (Zetasizer nano, Malvern Instruments) using a material refractive index of 1.590 and a dispersant (water at 25 °C) refractive index of 1.330. Within this paper, samples with a PDI > 0.4 were considered aggregated and were discarded.

The hybrid assemblies will from now on be labelled as follows: PxL_z where "Px" will be replaced with the abbreviation of the employed triblock copolymer and z represents the amount of added lipids in wt. %.

D. Quartz crystal microbalance with dissipation monitoring (QCM-D)

QCM-D measurements (Q-Sense E4, Sweden) were used to analyze the interaction of the hybrids with PLL coated surfaces. Silica-coated crystals (QSX300, Q-Sense) were cleaned by

TABLE II. Overview over the properties of the synthesized PChA macro RAFT agents ($PChA_{40}$ and $PChA_{21}$) and the ABA block copolymers P1-4.

Abbreviation	M_n PChA macroRAFT (kDa)	Hydrophilic extension	DP^{NMR}	M_n^{NMR} (kDa)	$Conversion^{NMR}$ (%)	M_n^{GPC} (kDa)
$PChA_{40}$	…	…	89	30.8	70	40.0
$PChA_{21}$	…	…	46	14.5	68	21.0
P1	40	NIPAAm	192	62	96	61
P2	21	NIPAAm	82	30	85	30
P3	21	NIPAAm	42	26	76	29
P4	21	PEG	117	77	65	…[a]

[a]It was not possible to analyse the polymer with GPC due to strong interactions with the column.

immersion in a 2 wt. % sodium dodecyl sulfate solution overnight and rinsing with Milli-Q water. Afterwards, the crystals were blow-dried with N_2, treated with UV/ozone for 20 min, and mounted into the liquid exchange chambers of the instrument. The frequency and dissipation measurements were monitored at $22 \pm 0.02\,^{\circ}\mathrm{C}$ or $37 \pm 0.02\,^{\circ}\mathrm{C}$. In all experiments, when a stable baseline in TRIS buffer was obtained, the silica-coated crystals were initially saturated with a pre-layer of PLL ($1\ \mathrm{mg\,ml^{-1}}$) before being washed with buffer. The coated crystals were then presented to hybrids, which were assembled with varying amounts of lipids (26–100 wt. %) and were let to adsorb until the crystal was saturated. Finally, the crystals were rinsed through with buffer and the frequency was allowed to stabilize. Normalized frequencies using the third harmonic are presented.

E. Cryo-electron microscopy (cryo-TEM)

Cryo-TEM samples were prepared by adsorbing 4 μl of the given sample onto Quantifoil R3.5/1 holey carbon film mounted on 300 mesh copper grids (Quantifoil Micro Tools GmbH, Jena, Germany). Prior to adsorption, the grid was rendered hydrophilic by glow discharge in a reduced atmosphere of air for 10 s. The specimen was applied and after 1 min incubation on the surface, the grid was blotted and quick-frozen in liquid ethane using a Vitrobot automated plunging device (FEI Company, Eindhoven, The Netherlands). Frozen grids were transferred to liquid nitrogen before loading into a Gatan 626 cryo-holder (Gatan, Pleasanton, CA, USA). The cryo-holder was then inserted into the stage of a Philips CM200 FEG TEM (FEI Company) operated at 200 kV. Imaging was performed at cryogenic temperatures (approximately $-170\,^{\circ}\mathrm{C}$) in low-dose, bright-field mode. Electron micrographs were recorded digitally on a TVIPS 4 k × 4 k CMOS Camera (TVIPS GmbH, Gauting Germany) at nominal defocus values of -2.5 μm.

F. Cell work

The RAW264.7 mouse macrophage cell line was used in all experiments. The cells were cultured in 75 $\mathrm{cm^2}$ flasks in medium (Dulbecco's Modified Eagle's Medium with $4500\ \mathrm{mg\,l^{-1}}$ glucose, sodium pyruvate and sodium bicarbonate supplemented with 10% fetal bovine serum, 2 mM L-glutamine, 50 $\mu\mathrm{g\ ml^{-1}}$ streptomycin and 50 $\mu\mathrm{g\ ml^{-1}}$ penicillin) at $37\,^{\circ}\mathrm{C}$ and 5% CO_2. The macrophages were scraped off the bottom of the flask with a cell scraper (BD Falcon), re-suspended in 5 ml media and counted.

For shear stress experiments, the cells were seeded into closed perfusion chambers (IbiTreat μ-slide VI0.4, Ibidi GmbH, Munich, Germany) at a density of 82 000 cells per channel in 120 μl medium and allowed to adhere at $37\,^{\circ}\mathrm{C}$ and 5% CO_2 for 24 h prior to the experiment. Hybrids made from 26 wt. % lipids and polymer (P1 and P2) loaded with 12 wt. % NBD-PC were diluted in media to reach the same fluorescent intensity. In static experiments ($\tau = 0$ dyn $\mathrm{cm^{-2}}$, τ_0), the cells were exposed to media containing hybrids in the same concentration for the desired time. In dynamic experiments, the hybrid-containing media was added to the reservoirs (syringes) of the Ibidi pumping system. The perfusion chamber was subsequently connected to a syringe pump and placed at $37\,^{\circ}\mathrm{C}$ and 5% CO_2. The flow experiments were conducted under these conditions with applied shear stress for either 2.5 h or 24 h. The cells were subsequently imaged with an Olympus IX81 inverted microscope prior to harvesting from the channels by treating with 100 μl trypsin for 5 min. The cell mean fluorescence (CMF) was assessed with a BD Accuri C6 flow cytometer using an excitation wavelength of 488 nm. At least 3000 cells were analyzed. The auto-fluorescence of the cells has been subtracted, and the control cells have been gated out in all presented results. All cell experiments have been conducted in at least three independent repeats. For confocal laser scanning microscopy (CLSM) imaging, the cells were fixed with a 4% paraformaldehyde solution and stained with DAPI and phalloidin. All images were taken with the same microscope settings using an inverted microscope coupled to an LSM 700 confocal laser scanning module (Zeiss, Germany). Cell viability of macrophages exposed to cell media with applied shear stresses ranging from 2 to 6 dyn $\mathrm{cm^{-2}}$ (τ_2, τ_4, and τ_6) for 24 h was assessed by using the commercial cell viability kit (CCK-8,

Sigma), which was added to the cells (10% CCK-8 in 200 μl cell media, 2 h). The absorbance was measured using a multimode plate reader and normalized to cells incubated at τ_0. The cell viability was statistically evaluated using a Student's T-test comparing samples with unequal variances.

The cell viability of macrophages exposed to the hybrids was determined using two commercially available counting kits (CCK-8 and FCCK, Sigma). The cells were seeded in the same density as in the flow chambers in 96 well plates and allowed to adhere for 24 h at 37 °C and 5% CO_2 before being exposed to $P2L_{26}$ for 24 h. The cell viability was determined either by absorbance measurements with the CCK-8 (10% CCK-8 in 200 μl cell media, 2 h). The second cell viability measurement was performed through fluorescent measurements by adding FCCK (0.2% in Dulbecco's modified PBS (Sigma), 1 h). The absorbance of the media (CCK-8) or fluorescence of the cells (FCCK) was measured by a multimode plate reader. These experiments were conducted in at least 3 independent repeats and the absorbance or fluorescence was normalized to untreated cells.

Except otherwise stated, all statistical analyses were carried out using a 2-way ANOVA with a confidence level of 95% ($\alpha = 0.05$), followed by a Tukey's multiple comparison posthoc test ($^*p < 0.05$) in the GraphPad Prism 6 software.

III. RESULTS AND DISCUSSION

A. Polymer synthesis

Inspired by our prior success to self-assemble polymersomes using a triblock copolymer with PChA as the hydrophobic part,[31] we synthesized different architectures of PNIPAAm-PChA-PNIPAAm (Scheme 2 and supplementary Figure S1).[40] The use of a bidirectional RAFT agent makes it possible to prepare well-defined ABA block copolymers whereby two arms of the polymer are formed simultaneously and (within the limits of polymer dispersity) are similar in size. The center of the block copolymers was designed to consist of poly(cholesteryl acrylate), a polymer which has previously been described in literature either as a homopolymer[32,33] or as a copolymer.[31,34–36] Cholesterol is a natural constituent of the cell membrane and is believed to confer a good biocompatibility making these polymers applicable in nanomedicine.[37]

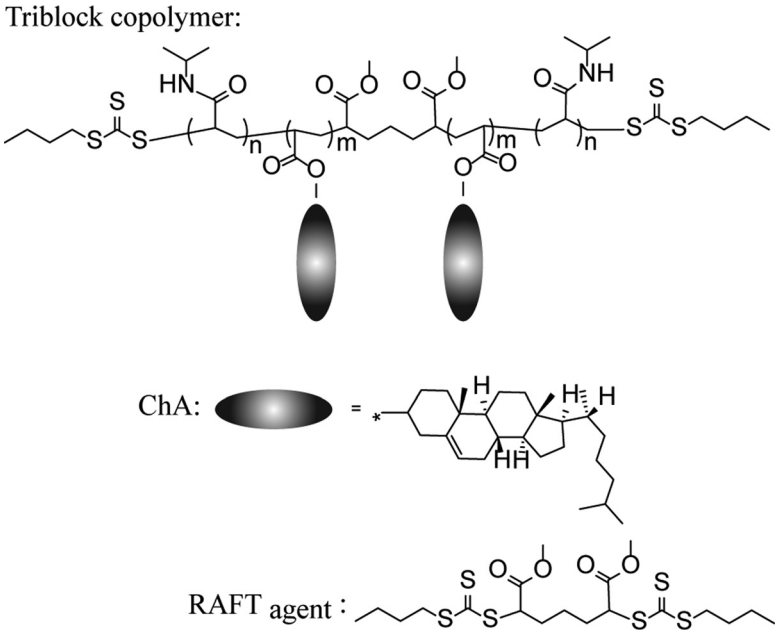

SCHEME 2. Chemical structure of a generic PNIPAAm-PChA-PNIPAAm block copolymer and the used RAFT agent.

PNIPAAm is one of the most well investigated polymers in biomedicine being thermo-responsive at physiologically relevant temperatures.[38] The lower critical solution temperature (LCST) of PNIPAAm is ∼34 °C in water and is used in these hybrids to alter their properties upon heating. In separate experiments, we also considered PEGA as hydrophilic extension as a comparison to the PNIPAAm-based block copolymers. PEG with linear polymer architecture is the golden standard in biomedicine and design of PEGA polymers as brush-type analogues to the linear counterpart are envisioned to broaden the scope and utility of this polymer in diverse biomedical applications.[39]

The step-wise synthesis of the ABA block copolymers by RAFT makes it possible to analyze the synthesized blocks independently. Dispersities for the block copolymers were analyzed by size exclusion chromatography and determined to be ∼1.1 for the PChA macro RAFT agent and all PNIPAAm containing block copolymers. We acknowledge hereby that it is unlikely that the column provided a fully satisfactory resolution of the species by molar mass yielding artificially low values for dispersity. At the same time, number-average molar mass values were consistent between GPC and ^{1}H-NMR. Macromolecular characteristics of the synthesized polymers are presented in Table II. We would like to note that the LCST of ABA block copolymers could not be determined since none of them were water soluble.

B. Lipid-polymer hybrid assemblies

With the aim to assemble thermo-responsive lipid-polymer hybrids, phospholipids were mixed with PNIPAAm-PChA-PNIPAAm copolymers in organic solvent and used to form a dried thin film of the mixed components. Decreasing amounts of lipids were added to the same amount of polymer in THF with the aim to identify the amount of lipids required to form vesicles which are stable in physiological buffer. The evaporation-hydration method, followed by extrusion though 200 nm filters, was considered for the assembly of the lipid-polymer hybrids. Hydration of the mixture in TRIS buffer was complete and only little residue on the walls of the flask suggested that all components were transferred into the aqueous phase—a behaviour not observed when block copolymers were used in the absence of lipids. The obtained hybrids were characterized using DLS (Table III). The used amounts of lipids between 100 wt. % and 26 wt. % led to comparable content of the assemblies in solution as estimated from the count rate of the DLS measurements using the same dilutions. If less than 26 wt. % lipids were used, only very few events were recorded indicating a low number of assemblies in solution. The diameter and PDI of the assemblies were compared to pristine liposomes (100 wt. % lipids, L_{100}). The PDI was independent of the used amount of lipids and PNIPAAm-PChA-PNIPAAm architecture. The diameter was found to decrease with decreasing

TABLE III. Diameter and PDI of the assembled lipid-polymer hybrids depending on the wt. % lipids and PNiPAAm-PChA-PNiPAAm triblock copolymer architecture after extrusion through 200 nm filters. The measurements were done at room temperature unless indicated otherwise.

Polymer	Lipids (wt. %)	Diameter (STD) (nm)	PDI (STD)
P1	71	211(3)	0.17(0.01)
	46	192(5)	0.14(0.03)
	26	149(27)	0.12(0.05)
P2	71	194(4)	0.17(0.05)
	46	182(26)	0.15(0.06)
	26	148(28)	0.14(0.07)
	26 (42 °C)	171(3)	0.11(0.04)
P3	71	205(9)	0.19(0.01)
	46	178(6)	0.12(0.02)
	26	161(2)	0.12(0.03)
L_{100}	100	188(5)	0.14(0.03)
	100 (42 °C)	189(3)	0.14(0.01)

amount of lipids in the mixture. Further, we measured the diameter and PDI of $P2L_{26}$ and L_{100} when cycling the temperature from 25 °C to 42 °C and back to 25 °C. For $P2L_{26}$ the diameter increased at the higher temperature. Upon cooling of the sample, the diameter returned to its starting value. On the other hand, L_{100} did not show any temperature dependent change in diameter. The PDI remained stable in all cases, showing that no aggregation occurred. These two findings were the first indication that the polymers and the lipids were assembled in hybrid structures. (We would like to note that the assembly of the block copolymers into polymersomes which were stable in PBS was unsuccessful using the described protocols. Refer to the supplementary material and Table S1 for more details.)[40]

Further, the ζ-potentials of $P1L_{26}$, $P2L_{26}$, and L_{100} were found to be comparable of ∼−5 mV. Finally, the $P2L_{26}$ assemblies were visualized by cryo-TEM as representative examples (Figure 1). Spherical assemblies of the expected size were observed, indicating that vesicular structures were assembled using the lipid-polymer mixture.

C. Adsorption of the lipid-polymer hybrids

With the aim to demonstrate that the different polymers co-assembled with the lipids, the adsorption characteristics of the lipid-polymer hybrids to a PLL pre-coated silica crystal were monitored by QCM-D and compared to the known high adsorption of liposomes to such a surface (Figure 2(a)). PLL was used as precursor layer to ensure that the liposomes did not rupture into supported lipid bilayers when interacting with the silica crystal. As expected at 22 °C, the measured change in frequency (Δf) and dissipation (ΔD, supplementary Figure S2)[40] of the crystals decreased with decreasing wt. % of lipids, likely due to the repelling nature of PNIPAAm at this temperature. Further, the assembly containing P3, the polymer with the shortest pending PNIPAAm chains, exhibited the largest decrease in Δf for higher lipid wt. % compared to the other two block copolymers. This result points towards the ability of the long PNIPAAm chains to hinder the adsorption to the PLL surface.

Following on, the $P1L_z$ assemblies were let to adsorb onto PLL coated crystals at 37 °C. Δf for PLL pre-coated crystals upon exposure to $P1L_{46}$ were found to be higher when the hybrids were adsorbed at 37 °C compared to 22 °C. This result was expected, since 37 °C is above the LCST of PNIPAAm and the hydrophobic nature of the polymer facilitated the deposition of the hybrids onto PLL coated substrates. This temperature dependent adsorption behaviour further supported the assembly of lipid-polymer hybrid structures. With the aim to confirm that this observation was PNIPAAm specific, hybrids using P4 as the polymer building block and 26 wt. % lipids were assembled. The PEG-based block copolymer was not expected to exhibit temperature dependent adsorption behaviour as found for the PNIPAAm-based hybrids. Further, only this lipid-copolymer combination was assembled, since the highest tested amount of polymer was expected to show the property best. The diameter and PDI of $P4L_{26}$ hybrids were similar as for the PNIPAAm-based assemblies (supplementary Table S2).[40] The exposure of $P4L_{26}$-based hybrids to PLL coated crystals led to similarly low Δf independent on the used deposition

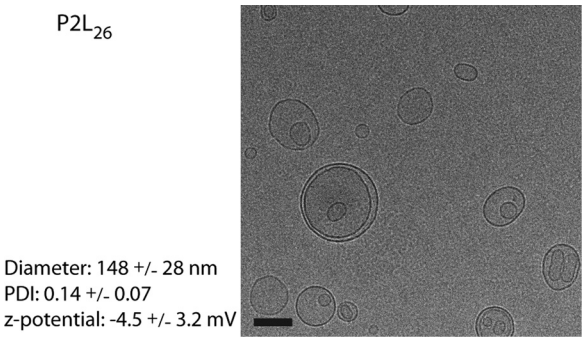

FIG. 1. Cryo-TEM image of hybrid assemblies $P2L_{26}$, including diameter, PDI, and ζ-potential assessed by DLS. The scale bar is 100 nm.

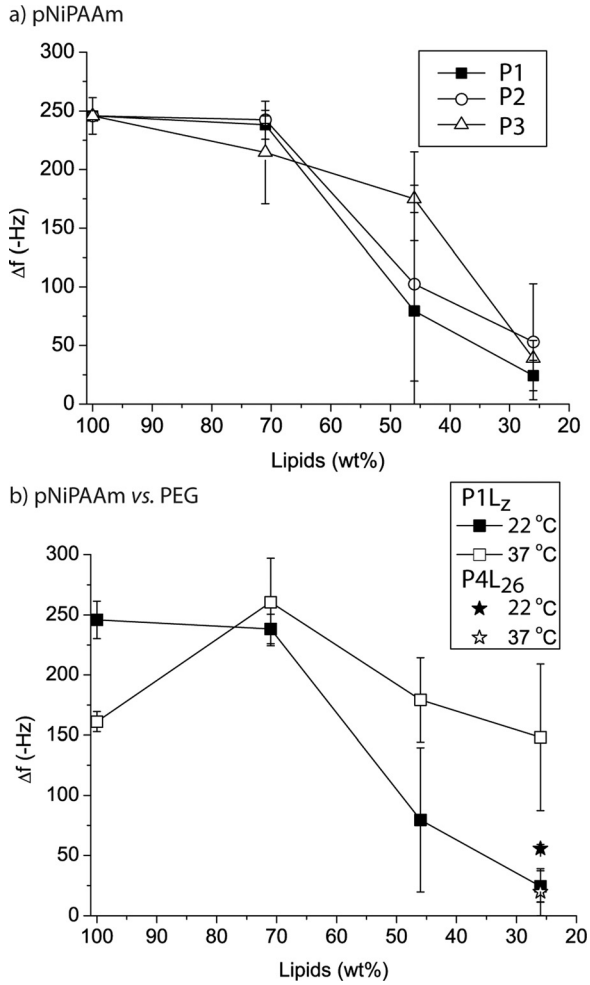

FIG. 2. Adsorption of hybrid assemblies: (a) Frequency changes Δf of PLL coated crystals upon exposure to hybrid assemblies made from different types of PNIPAAm-based triblock copolymers and lipids in different ratios in TRIS buffer at 22 °C. (b) Frequency changes Δf of PLL coated crystals upon exposure to P1L$_z$ or P4L$_{26}$ in TRIS buffer at 22 °C and 37 °C.

temperature. Further, to ensure that the low Δf was due to the repelling nature of the polymers in the hybrids and not only because of the low concentration of liposomes in solution due the small amount of lipids used, liposomes were assembled using only 0.18 mg ml^{-1} lipids (as compared to the regular 2.5 mg ml^{-1}). $\Delta f = -208.7 \pm 2.9$ Hz was measured for PLL pre-coated crystals exposed to these liposomes. This was a ∼8× higher Δf as measured for PxL$_{26}$. The above two mentioned aspects further substantiate our hypothesis that thermo-responsive lipid-polymer hybrids were assembled.

D. Interaction of the hybrids with macrophages

With the aim to understand if these hybrid assemblies have potential as drug carriers, we biologically evaluated a representative hybrid, P2L$_{26}$, in terms of uptake efficiency and cytotoxicity. Macrophages were chosen for this purpose since every intravenously administered delivery vehicle will come into contact with this cell type, and they are important to be considered for vaccine applications.

First, we assessed the CMF (Figure 3(a)) and uptake efficiency (supplementary material Figure S3)[40] of macrophages upon incubation with fluorescently labelled hybrids depending on the exposure time at static conditions ($\tau_0 = 0$ dyn cm^{-2}). The fluorescent hybrids were obtained

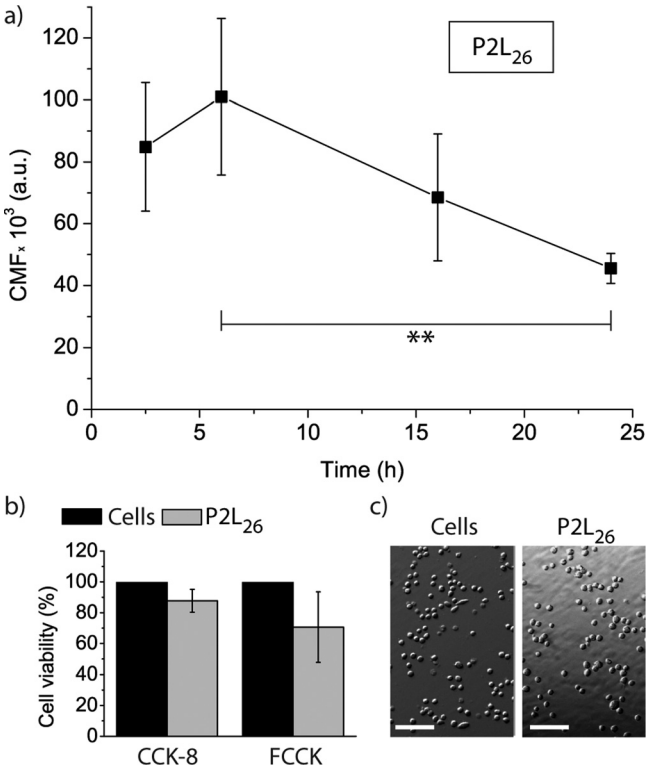

FIG. 3. (a) Time dependent evolution of the CMF of macrophages exposed to $P2L_{26}$ at τ_0. ($n = 4$, $^{**}p < 0.01$). (b) Cell viability of macrophages exposed to $P2L_{26}$ for 24 h at τ_0 normalized to untreated cells. (c) Representative bright field images of macrophages in the absence or presence of $P2L_{26}$ at τ_0 for 24 h. The scale bars are 50 μm.

by adding fluorescent lipids. The CMF reached the maximum between 2.5 and 6 h and subsequently significantly decreased between 6 h and 24 h for the chosen concentration of hybrids. The uptake efficiency remained similar for the tested conditions. This observation pointed towards a fast initial uptake probably followed by intracellular degradation of the fluorophore by the macrophages.

Next, the cytotoxicity of the $P2L_{26}$ assemblies on the macrophages within 24 h was assessed and compared to untreated cells at τ_0 (Figure 3(b)). Using the commercial CCK-8 and FCCK assays, we found no significant differences in cell viability compared to the control cells. Visual inspection of cell density and health with bright field microscopy supported the measured similar cell viability (Figure 3(c)).

Following on, the short-term interaction of $P2L_{26}$ and $P1L_{26}$ with macrophages with applied shear stress was assessed in a microfluidic setup. Shear stress is an important mechanical factor present *in vivo* caused by the blood flow. Since macrophages are semi-adherent cells, and since we have previously observed that applied shear stress reduced the number of surface-adherent macrophages,[28] the number of adherent cells in the channels depending on the applied shear stress and time was compared (Figure 4). The results were normalized to cells adhering in the absence of shear stress after either 2.5 h or 24 h. Analysing the macrophages after 24 h revealed that the number of cells significantly increased for τ_2 ($\tau_2 = 2$ dyn cm^{-2}) compared to τ_0. Moreover, there was a significant increase in cell viability at τ_2 from 2.5 h to 24 h, demonstrating that the cells proliferate in the presence of shear stress. When further increasing the shear stress to τ_4 ($\tau_4 = 4$ dyn cm^{-2}) and τ_6 ($\tau_6 = 6$ dyn cm^{-2}), the number of macrophages decreased after 24 h and 2.5 h, respectively, compared to τ_0 as shown by the representative bright field images (Figure 4). These findings, which were not surprising due to the semi-adherent nature of the cells, indicated that the shear stress dependent adhesion of macrophages

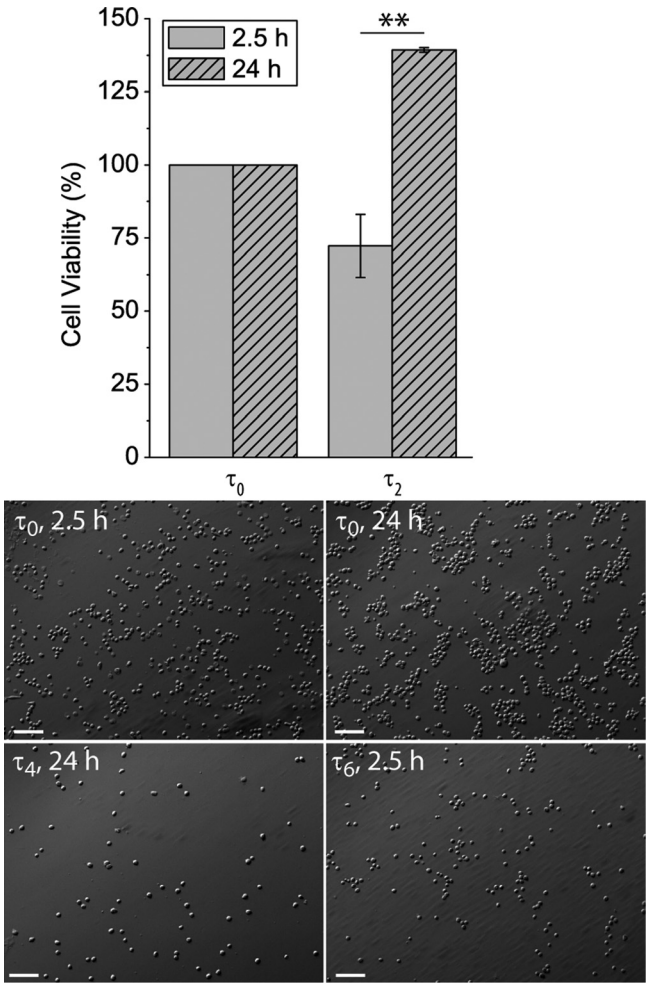

FIG. 4. Cell viability of macrophages exposed to τ_0 or τ_2 for either 2.5 h or 24 h. The data have been normalized to the results at τ_0 ($n = 4$, $^{**}p < 0.01$). Representative bright field images of macrophages exposed to τ_0 for 2.5 h and 24 h (top) as well as τ_4 for 24 h and τ_6 for 2.5 h, respectively (bottom). The scale bars are 100 μm.

was an important aspect to consider when employing this cell type for the *in vitro* assessment of potential drug carriers and therapeutic compounds.

With the aim to understand to what extent applied shear stress affected the uptake/association of macrophages with the fluorescent hybrid assemblies, the normalized CMF (Figure 5(a)) and the uptake efficiency (supplementary material Figure S4)[40] were assessed after 2.5 h with applied shear stress (τ_4) compared to τ_0. Cells grown in the absence of the hybrids at τ_0 were used to normalize the CMF. The uptake efficiency was independent on the chosen hybrids and the applied shear stress. Further, the CMF of macrophages exposed to $P2L_{26}$ was significantly lower at τ_0 compared to τ_4, i.e., the applied shear stress increased the uptake of the hybrids. On the other hand, there was no significant difference in CMF depending on the applied shear stress for cells incubated with $P1L_{26}$. At τ_0, the CMF was similar for cells exposed to $P2L_{26}$ and $P1L_{26}$, while at τ_4, the CMF was significantly lower in the latter case. These findings indicated that the PNIPAAm extensions affected the ability of the cells to interact with the hybrids, i.e., higher MW extensions reduced the uptake. The hybrids in the used concentration did not inherently affect the cell viability (Figure 5(b)). The reduced number of macrophages at τ_4 was likely due to the applied shear stress and not due to the presence of the hybrids, as previously discussed in Figure 4. Further, the internalization of the hybrids was confirmed by CLSM (Figure 5(c)). The green signal due to the

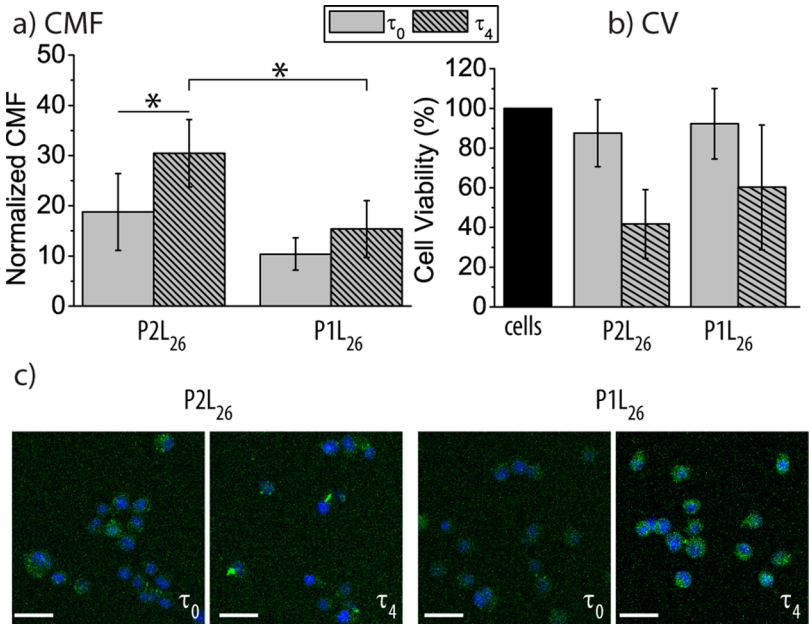

FIG. 5. (a) CMF of macrophages after 2.5 h treatment with $P2L_{26}$ or $P1L_{26}$ at τ_4 compared τ_0. ($n = 4$, $*p < 0.05$). (b) Cell viability of macrophages after 2.5 h treatment with $P2L_{26}$ or $P1L_{26}$ at τ_4 compared to τ_0. (c) Representative CLSM images of macrophages after 2.5 h treatment with $P2L_{26}$ or $P1L_{26}$ at τ_4 compared τ_0. The scale bars are 25 μm.

uptake of the green fluorescent lipids was homogenously distributed in the cytosol, but was excluded from the nuclei.

IV. CONCLUSIONS

We report the successful synthesis of novel PNIPAAm-PChA-PNIPAAm block copolymers and their assembly in lipid-polymer hybrids with phospholipids. The adsorption of these hybrids to a PLL coated surface was dependent on the amount of lipids present and the deposition temperature. It was found that the number of adhering macrophages depended on the applied shear stress and exposure time, i.e., increasing the shear stresses up to τ_2 led to higher numbers of adhering cells, followed by a decrease due their washing off in the presence of higher shear stress. Further, the CMF of macrophages exposed to these hybrids was highest for short PNIPAAm extensions with applied shear stress. Under the tested conditions, there was no inherent negative effect on the macrophage viability due to the presence of the hybrids.

In summary, the cell culture analysis of the novel type of hybrids with preserved temperature responsiveness is considerably contributing to the development of this type of nano-sized vesicles as potential drug delivery vehicles.

ACKNOWLEDGMENTS

This work was supported by a Sapere Aude Starting Grant from the Danish Council for Independent Research, Technology and Production Sciences, Denmark.

[1]K. Miyata, R. J. Christie, and K. Kataoka, React. Funct. Polym. **71**, 227 (2011).
[2]J. S. Lee and J. Feijen, J. Controlled Release **161**, 473 (2012).
[3]T. M. Allen and P. R. Cullis, Adv. Drug Delivery Rev. **65**, 36 (2013).
[4]V. P. Torchilin, Nat. Rev. Drug Discovery **4**, 145 (2005).
[5]S. Hauschild, U. Lipprandt, A. Rumplecker, U. Borchert, A. Rank, R. Schubert, and S. Förster, Small **1**, 1177 (2005).
[6]B. M. Discher, Y.-Y. Won, D. S. Ege, J. C.-M. Lee, F. S. Bates, D. E. Discher, and D. A. Hammer, Science **284**, 1143 (1999).
[7]C. LoPresti, H. Lomas, M. Massignani, T. Smart, and G. Battaglia, J. Mater. Chem. **19**, 3576 (2009).
[8]A. Rösler, G. W. M. Vandermeulen, and H.-A. Klok, Adv. Drug Delivery Rev. **64**, 270 (2012).
[9]J. F. Le Meins, C. Schatz, S. Lecommandoux, and O. Sandre, Mater. Today **16**, 397 (2013).

[10]M. Chemin, P.-M. Brun, S. Lecommandoux, O. Sandre, and J.-F. Le Meins, Soft Matter **8**, 2867 (2012).
[11]T. Ruysschaert, A. F. P. Sonnen, T. Haefele, W. Meier, M. Winterhalter, and D. Fournier, J. Am. Chem. Soc. **127**, 6242 (2005).
[12]A. Olubummo, M. Schulz, B.-D. Lechner, P. Scholtysek, K. Bacia, A. Blume, J. Kressler, and W. H. Binder, ACS Nano **6**, 8713 (2012).
[13]M. Schulz, D. Glatte, A. Meister, P. Scholtysek, A. Kerth, A. Blume, K. Bacia, and W. H. Binder, Soft Matter **7**, 8100 (2011).
[14]Z. Cheng and A. Tsourkas, Langmuir **24**, 8169 (2008).
[15]Z. Cheng, D. R. Elias, N. P. Kamat, E. D. Johnston, A. Poloukhtine, V. Popik, D. A. Hammer, and A. Tsourkas, Bioconjugate Chem. **22**, 2021 (2011).
[16]J. Nam, P. A. Beales, and T. K. Vanderlick, Langmuir **27**, 1 (2011).
[17]J. Nam, T. K. Vanderlick, and P. A. Beales, Soft Matter **8**, 7982 (2012).
[18]N. Pippa, E. Kaditi, S. Pispas, and C. Demetzos, Soft Matter **9**, 4073 (2013).
[19]T. Bhowmick, E. Berk, X. Cui, V. R. Muzykantov, and S. Muro, J. Controlled Release **157**, 485 (2012).
[20]O. C. Farokhzad, A. Khademhosseini, S. Jon, A. Hermmann, J. Cheng, C. Chin, A. Kiselyuk, B. Teply, G. Eng, and R. Langer, Anal. Chem. **77**, 5453 (2005).
[21]C. Fillafer, G. Ratzinger, J. Neumann, Z. Guttenberg, S. Dissauer, I. K. Lichtscheidl, M. Wirth, F. Gabor, and M. F. Schneider, Lab Chip **9**, 2782 (2009).
[22]T. Fujiwara, H. Akita, K. Furukawa, T. Ushida, H. Mizuguchi, and H. Harashima, Biol. Pharm. Bull. **29**, 1511 (2006).
[23]S. S. Harris and T. D. Giorgio, Gene Ther. **12**, 512 (2005).
[24]B. Prabhakarpandian, M.-C. Shen, K. Pant, and M. F. Kiani, Microvasc. Res. **82**, 210 (2011).
[25]M. Godoy-Gallardo, P. K. Ek, M. M. T. Jansman, B. M. Wohl, and L. Hosta-Rigau, Biomicrofluidics **9**, 052605 (2015).
[26]B. M. Teo, R. van der Westen, L. Hosta-Rigau, and B. Städler, Biochim. Biophys. Acta, Gen. Subj. **1830**, 4838 (2013).
[27]L. Hosta-Rigau and B. Städler, Mol. Pharmaceutics **10**, 2707 (2013).
[28]K. Panneerselvam, S. Mena-Hernando, B. M. Teo, K. N. Goldie, and B. Stadler, RSC Adv. **4**, 44769 (2014).
[29]L. Castro-Nunez, I. Dienava-Verdoold, E. Herczenik, K. Mertens, and A. B. Meijer, J. Thromb. Haemostasis **10**, 1929 (2012).
[30]N. Wohner, P. Legendre, C. Casari, O. D. Christophe, P. J. Lenting, and C. V. Denis, J. Thromb. Haemostasis **13**, 815 (2015).
[31]L. Hosta-Rigau, B. E. B. Jensen, K. S. Fjeldsø, A. Postma, G. Guoxin Li, K. N. Goldie, F. Albericio, A. N. Zelikin, and B. Städler, Adv. Healthcare Mater. **1**, 791 (2012).
[32]A. C. De Visser, K. De Groot, J. Feyen, and A. Bantjes, J. Polym. Sci., Part A-1: Polym. Chem. **9**, 1893 (1971).
[33]A. C. de Visser, J. Feyen, K. de Groot, and A. Bantjes, J. Polym. Sci., Part B: Polym. Lett. **8**, 805 (1970).
[34]F. Delbecq and K. Kawakami, Colloids Surf., A **444**, 173 (2014).
[35]S.-J. He, Y. Zhang, Z.-H. Cui, Y.-Z. Tao, and B.-L. Zhang, Eur. Polym. J. **45**, 2395 (2009).
[36]H. Zeng, Y. Li, H. Zhang, and X. Wang, Acta Polym. Sin. **1**, 327 (2004).
[37]L. Hosta-Rigau, Y. Zhang, B. M. Teo, A. Postma, and B. Stadler, Nanoscale **5**, 89 (2013).
[38]L. Klouda and A. G. Mikos, Eur. J. Pharm. Biopharm. **68**, 34 (2008).
[39]E. M. Pelegri-O'Day, E.-W. Lin, and H. D. Maynard, J. Am. Chem. Soc. **136**, 14323 (2014).
[40]See supplementary material at http://dx.doi.org/10.1063/1.4929405 for the chemical structures, the polymersome assembly, dissipation changes, DLS results of hybrid assemblies, and the uptake efficiencies.